angle as before we find

$$\langle|(0|r|1)|^2\rangle_{Av}=\frac{W^2A^2}{M^2\omega^4}\frac{c^2d^2R^2}{c^2(a^2+b^2)}\left[\frac{1}{d(c+d)}\frac{\gamma^2}{cd}\right], \quad \text{(A16)}$$

where $\gamma^2=c^2/(a^2+b^2)$.

Thus, the cross section is increased over that for the square well by the factor

$$[R/(R-R_0)][1+c(c+d)/(a^2+b^2)]. \quad \text{(A17)}$$

To compare the modified cross sections with experiment, we must choose a value for R_0. We choose $R_0=R/4$, since then the $2s$ level is pushed up near the top of the distribution for Z near 45, as required by the angular distributions of Rh and Ag photoprotons. For this value of R_0 the depth of the well need not be increased substantially over that of the square well. We then find, for the parameters chosen in the text, an increase in the cross section by a factor of 3.7 as compared with (9). This asymptotic estimate is, however, good only for $l=0$ or 1, since it is predicated on the assumption $aR_0>l$. For higher values of l the change in the cross section will be less pronounced, since the wave functions do not differ as much from those for the square well.

PHYSICAL REVIEW VOLUME 82, NUMBER 5 JUNE 1, 1951

Photoprotons from Magnesium

M. ELAINE TOMS AND WILLIAM E. STEPHENS
Department of Physics, University of Pennsylvania, Philadelphia, Pennsylvania

(Received February 9, 1951)

The distributions in energy and in angle of the protons ejected from magnesium by the bremsstrahlung x-rays of a 24-Mev betatron have been observed in nuclear emulsions. Both normal magnesium and enriched Mg^{25} show a uniform angular distribution for all proton energies. The energy distribution of the protons from enriched Mg^{25} is compared to the distributions calculated from an evaporation process using various energy level densities. Good agreement is obtained using the known Na^{24} level densities. The integrated cross section of the $Mg^{25}(\gamma,p)$ reaction is determined as 0.056 ± 0.03 Mev-barn.

I. INTRODUCTION

EARLY measurements[1] of the ratio of (γ,p) to (γ,n) cross sections have indicated larger values than expected from the statistical theory of nuclei.[2] The observation of a broad resonance in the photoexcitation curves was also surprising.[3–5] The explanations[6,7] which were advanced for these phenomena seemed to differ in the angular and energy distributions to be expected of the ejected protons. Consequently, this investigation was initiated to examine such characteristics of the photoprotons in the hope that they would help determine the predominant mechanisms. Magnesium was chosen as the first element to be investigated since its photoproton yield was known to be appreciable.[1,5] Initial results on the angular distribution of photoprotons from normal magnesium indicated no appreciable direct photoelectric effects.[8] Enriched magnesium was secured from the AEC, and further work was undertaken to refine the observations. Meanwhile other experimental data[9,10] and theoretical calculations[11–15] have been published.

II. APPARATUS

The x-ray beam from an Allis-Chalmers betatron is defined, as shown in Fig. 1, by a collimator which has about 16 in. of lead plus 16 in. of steel and lead with a magnetic field to remove the electrons. The x-ray beam which emerges from the collimator is $\frac{1}{4}$ in. in diameter and is diverging at an angle of only eleven minutes. The shielding afforded by the collimator is at least a factor of 10^4 between the beam intensity and the stray radiation. A concrete wall 16 to 24 in. thick surrounds the collimator to reduce the neutron background. Under normal running conditions, the beam intensity at the camera is about 25 roentgens/min as measured by a Victoreen and has passed through 0.7 cm of

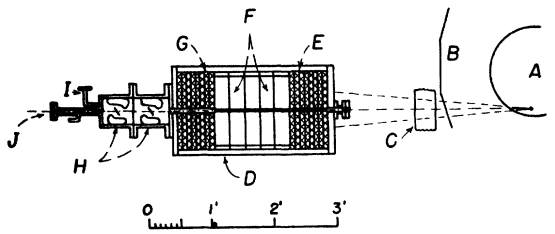

FIG. 1. Experimental arrangement showing A—betatron doughnut, B—coil box, C—monitor, D—collimator, E and G—lead collimating disks, F—steel and lead disks holding Alnico magnets, H—double camera, I—to vacuum pump, and J—window.

[1] O. Hirzel and H. Wäffler, Helv. Phys. Acta **20**, 373 (1947).
[2] V. F. Weisskopf and D. H. Ewing, Phys. Rev. **57**, 472, 935 (1940).
[3] G. C. Baldwin and G. S. Klaiber, Phys. Rev. **73**, 1156 (1948).
[4] M. L. Perlman and G. Friedlander, Phys. Rev. **74**, 422 (1948).
[5] McElhinney, Hanson, Becker, Duffield, and Diven, Phys. Rev. **75**, 542 (1949).
[6] L. I. Schiff, Phys. Rev. **73**, 1311 (1948).
[7] M. Goldhaber and E. Teller, Phys. Rev. **74**, 1046 (1948).
[8] Toms, Halpern, and Stephens, Phys. Rev. **77**, 753(A) (1950).
[9] Curtis, Hornbostel, Lee, and Salant, Phys. Rev. **77**, 290 (1950).
[10] B. C. Diven and G. M. Almy, Phys. Rev. **80**, 407 (1950).
[11] E. D. Courant, Phys. Rev. **74**, 1226(A) (1948); and private communications.
[12] P. Jensen, Naturwiss. **35**, 190 (1948).
[13] L. Wolfenstein, Phys. Rev. **78**, 322(A) (1950).
[14] J. S. Levinger and H. A. Bethe, Phys. Rev. **78**, 115 (1950).
[15] K. J. LeCouteur, Proc. Phys. Soc. (London) **63**, 259 (1950).

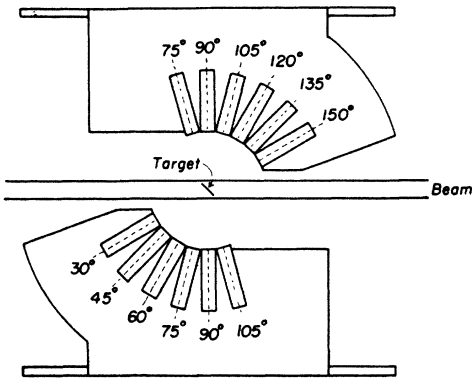

FIG. 2. The nuclear emulsion plate holders showing the positions of the plates.

aluminum and one cm of porcelain. The camera is bolted onto the collimator, and both are evacuated to a pressure of about 100 microns of mercury. The alignment of the beam with the camera and collimator is checked by exposing x-ray film to the beam at the end of the collimator and at the end of the camera. A cylindrical shell slides inside the camera and carries the plate holders and the foil support. Ilford C-2, 100μ-emulsions are cut to $1\times\frac{1}{4}$ in., and the edges are painted with dilute Duco cement to avoid peeling. These plates are cemented to the Lucite supports at $\frac{15}{16}$ in. from the target and $\frac{9}{32}$ in. below the center of the beam, and are set at various angles to the beam as shown in Fig. 2. The camera is shielded from stray radiation by 2 in. of lead piled around it.

The plates are processed by a constant temperature development. After fixing and washing, the plates are soaked in a one percent solution of glycerine to prevent peeling later. After drying, the plates are removed from their supports, remounted in a holder, and examined under a Spencer binocular microscope using 10× oculars and a 97× objective with oil immersion. The green lines from a mercury arc are used for illumination. Similarly situated regions in each plate are scanned and the proton tracks measured only when they enter the top surface of the emulsion and have the correct angle and dip to have come from the target, as determined from their initial 10 μ of path. The allowed angles are 0° to ±12° and 4° to 21° dip. Horizontal and vertical lengths are measured on all acceptable tracks and the real lengths calculated using corrections for emulsion shrinkage and microscope calibration. Half the effective foil thickness in emulsion distance is added to each track and the energy determined from the Ilford range-energy curve.[16]

TABLE I. Magnesium isotopes, thresholds, and cross sections.

	Mg^{24}		Mg^{25}		Mg^{26}	
Isotope abundances						
Normal	0.784		0.102		0.114	
Enriched	0.107		0.868		0.025	
	$-Q$	$\sigma_{17.5}$	$-Q$	$\sigma_{17.5}$	$-Q$	$\sigma_{17.5}$
(γ, n)	16.8 Mev	0.001 barn	6.8 Mev		11.2 Mev	
(γ, p)	12.3		10.6	0.00283 barn	14.2	0.00156 barn
(γ, d)			16			
(γ, np)			18.2			
(γ, α)	10		9		10	
		$\sigma_{RaBe\,n}$				
(n, p)	2	0.1 barn				

The background was estimated in two ways. In several sample regions, all tracks in the emulsion were counted and all those which entered the surface were observed for angle and dip. The tracks coming in a direction other than from the foil were roughly random in their direction and point of origin. (90 tracks in 1.4 mm^2.) Those originating in the emulsion were presumably neutron recoils. Those entering the surface most probably were scattered protons but may also have been neutron recoils. Assuming that these tracks contributed to the background by originating, by chance, in the top two microns of the emulsion and having, also by chance, the correct direction to have originated in the foil gives a background of 0.035 tracks in 1.4 mm^2 compared to an average number of protons from the foil of 26.5 tracks in 1.4 mm^2 or approximately 0.1 percent. Another check on the background was afforded by a separate run with a gold foil in the beam. A sample scanning of the nuclear emulsions yielded a few random tracks, 24 in 0.4 mm^2, but none entering the surface with the correct direction.

A correction was necessary for otherwise good tracks which emerged from the emulsion before stopping. These tracks were corrected by increasing the length of each to the average length of all tracks longer than it. In order to check this correction a geometric factor was calculated for the fraction of tracks expected to go through the emulsion at each energy. Applying this to the corrected distribution gave the number expected to go through. The observed number, 138, is somewhat greater than the calculated number, 98, but the difference is not much greater than the statistical fluctuations and uncertainties in the geometry.

Protons from magnesium can be caused by several transmutations. Table I gives the relative abundances of the three magnesium isotopes and the thresholds for the various possible phototransmutations together with cross sections, where known. The photocross sections were determined with 17.5-Mev gamma-rays and the neutron cross section with radium beryllium neutrons.

It might be expected that the Mg^{24} reactions would be predominate with normal magnesium foil. In order to investigate the possibility of protons from $Mg^{24}(n,p)Na^{24}$ reaction produced by neutrons from the betatron, a sample of magnesium was irradiated first in the direct x-ray beam and then just out of the beam. The background neutron intensity would be expected to be approximately the same at each position. Appreciable

[16] Lattes, Fowler, and Cuer, Proc. Phys. Soc. (London) **59**, 883 (1947).

Na^{24} activity was observed when the magnesium was exposed in the x-ray beam (due to the $Mg^{25}(\gamma,p)Na^{24}$) but none (less than one percent of the activation in the beam) when the magnesium was out of the beam. As an additional check the number of neutrons from the betatron with energies (>2 Mev) sufficient to activate Si^{31} by $P^{31}(n,p)Si^{31}$ was determined by observing the Si^{31} activation near the betatron. A RaBe source whose neutron emission could be calculated was also used to produce both $P^{31}(n,p)Si^{31}$ and $Mg^{24}(n,p)Na^{24}$ reactions. From these observations, it was calculated that about 10^9 neutrons/sec came from the betatron and 2×10^3 n/sec/cm^2 would be expected to be in the collimated x-ray beam at the foil. A considerable number of neutrons, of the order of 4×10^7 n/sec, are produced by the stopping of the x-rays in the collimator,[17] but the camera was shielded from most of these neutrons. From the activation in the normal magnesium of $Mg^{24}(n,p)Na^{24}$ by the RaBe neutrons and the $Mg^{25}(\gamma,p)Na^{24}$ from the betatron, it was estimated that 6×10^5 neutrons/sec/cm^2 would produce the same amount of activation (and hence equal numbers of protons) as the betatron x-ray beam. Consequently, the (n,p) reactions are considered negligible.

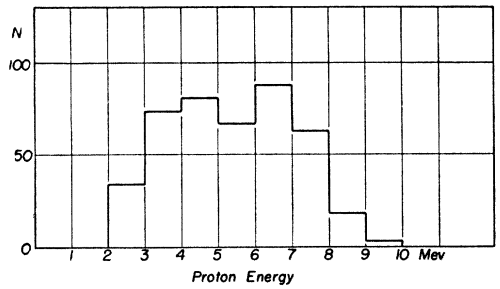

FIG. 3. Energy distribution of the proton tracks observed with normal magnesium foil at a betatron energy of 22.5 Mev.

III. MEASUREMENTS

The first exposure totaled 7000 roentgens on a 2.77-mil thick (12.2-mg/cm^2) magnesium metal foil. The betatron was run at a nominal energy of 22.5 Mev. Equal areas, 2 mm wide by 12 mm long, were scanned on plates situated at 30°, 60°, 120°, and 150°. Half this area was scanned on each of the opposite 90° plates. The agreement between these opposite plates checked the alignment and centering of the beam. The energy distribution of the 423 measured tracks is shown in Fig. 3. The foil half-thickness, which is the uncertainty in the proton range, is equivalent to about $\frac{2}{3}$ Mev for 2-Mev protons and about 0.2 Mev for 10-Mev protons. The angular distribution of these tracks is indicated in Fig. 4. The vertical lines are the statistical uncertainty, while the horizontal lines through each point indicate the angular spread allowed.

[17] J. S. Levinger, Nucleonics 6, No. 5, 64 (1950).

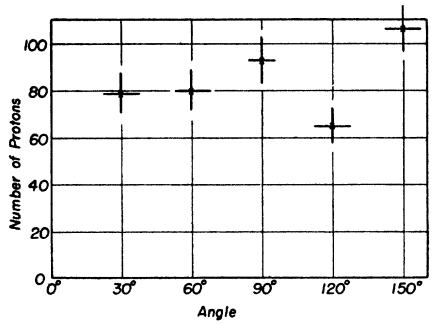

FIG. 4. Angular distribution of the proton tracks observed with a normal magnesium foil at a betatron energy of 22.5 Mev.

In order to improve the statistics and refine the measurements, a foil of enriched magnesium was prepared. Magnesium oxide containing 86.8 percent of Mg^{25} with only 2.5 percent of Mg^{26} and 10.7 percent of Mg^{24} was kindly loaned us by the Isotopes Division of the AEC. Forty milligrams of this magnesium oxide was reduced with aluminum in a vacuum and the resulting lump of magnesium metal rolled into a foil 2.2 mils thick (9.62 mg/cm^2) and about one centimeter square. Spectroscopic tests indicated negligible amounts of aluminum in the magnesium metal. This enriched foil was exposed to 36,900 roentgens of the bremsstrahlung x-rays from 24-Mev electrons hitting the platinum target of the betatron donut. An area 1 mm by 10 mm was scanned on plates at 30°, 60°, 90°, 120°, and 150°. This same area was scanned on the appropriate plates at 75° and 105°. No significant differences in the number of tracks found on opposite plates at 75°, 90°, and 105° again confirmed the beam alignment. The energy and angular distributions are shown in Figs. 5 and 6. The uncertainty in proton

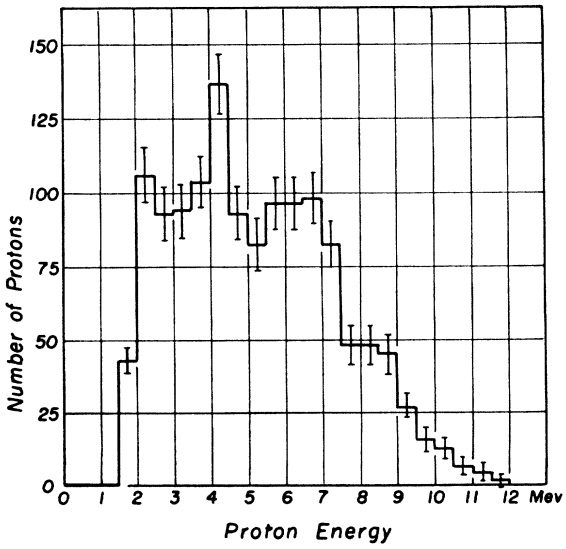

FIG. 5. Energy distribution of the proton tracks observed with enriched Mg^{25} foil at a betatron energy of 24 Mev.

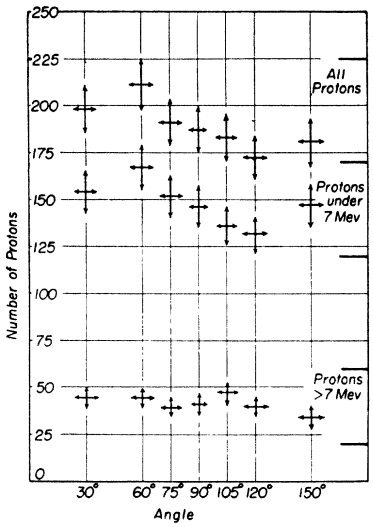

FIG. 6. Angular distribution of the proton tracks observed with enriched Mg^{25} foil at a betatron energy of 24 Mev.

energy (equivalent to half the foil thickness) for the enriched foil varies from ± 0.15 Mev for the 10-Mev protons to ± 0.5 Mev for the 2-Mev protons at the best angles. In Fig. 6 the angular distribution of the protons with energies greater than 7 Mev and less than 7 Mev is shown in addition to the totals.

In order to compute the expected energy distribution of the protons we have measured the yield curve of the $Mg^{25}(\gamma,p)Na^{24}$ reaction in ordinary magnesium by observing the 15-hour half-life of Na^{24} activated at different betatron energies. The activation counting rate per unit x-ray intensity is plotted in Fig. 7 as a function of the nominal betatron energy. This yield curve was reduced to a relative cross-section curve by the use of normalized bremsstrahlung curves.[18] The relative cross-section curve is shown in Fig. 8. Only the statistical errors carried over from the differentiation of the yield curve are indicated.

In order to compute the absolute cross section of the photoproton reactions we have evaluated the solid angle of the nuclear emulsions in two ways. Using the measured geometry we calculate a fractional solid angle for the area scanned in the nuclear emulsion to be $\omega_n = 3\times 10^{-4}$ for the normal magnesium exposure and $\omega_e = 2\times 10^{-4}$ for the enriched magnesium run. This solid angle was also determined by counting the alpha-particle tracks in the nuclear emulsions coming from a polonium alpha-source substituted for the magnesium foil. The alpha-source was calibrated in a flow counter of essentially 2π-geometry. The solid angles measured in this fashion were $\omega_n = 3.48\times 10^{-4}$ for 0.24 cm^2 scanned, and $\omega_e = 1.95\times 10^{-4}$ for 0.1 cm^2 scanned. Then the yield of photoprotons is taken to be:

$$ANtR\int_0^{E_{\max}} n(E, E_{\max})\sigma(E)dE = P/\omega,$$

where P/ω is the number of protons ejected from the foil by R roentgens, A is the area of the x-ray beam, t is the thickness of the foil in the direction of the beam, N is the number of nuclei per cc, n is the number of photons/Mev interval/cm^2/roentgen unit, when the betatron is run at an energy of $E_{\max}$, σ is the photoproton cross section for photons of energy E, and P is the number of protons observed in the nuclear emulsions when an area, a, constituting a fractional solid angle of ω is scanned. The integral is the yield per atom per roentgen unit.

$$y = \int_0^{E_{\max}} n(E, E_{\max})\sigma(E)dE = P/ANtR\omega.$$

Multiplying by Avogadro's number gives Y, the yield per mole per roentgen unit. We have used n from Katz's[18] curves and calculated the absolute cross sections from the observed yields. The data involved in the calculation of the yield from the enriched foil are: $N = 4.2\times 10^{22}$ nuclei of Mg/cc, $t = 7.9\times 10^{-3}$ cm, $A = 0.267$ cm^2, $\omega_e = 2\times 10^{-4}$ for 0.1 cm^2 scanned, and $P = 190$ protons in 0.1 cm^2 scanned. Thus, $y = 2.92\times 10^{-19}$ photoprotons/atom/roentgen, and $Y = 1.75\times 10^5$ protons/mole/roentgen for the enriched magnesium. The uncertainty in this yield is estimated to be of the order of 50 percent. A similar calculation for the normal magnesium foil gives a yield of about 3.1×10^{-19} protons/nucleus of magnesium/roentgen or 18.6×10^4 protons/mole/roentgen at a maximum betatron energy of 22.5 Mev. This yield is somewhat less certain than that for the enriched foil due to inaccuracies in the ionization chamber monitor integrator readings and is estimated as ± 75 percent. Taking into account the relative abundances of the magnesium isotopes in the

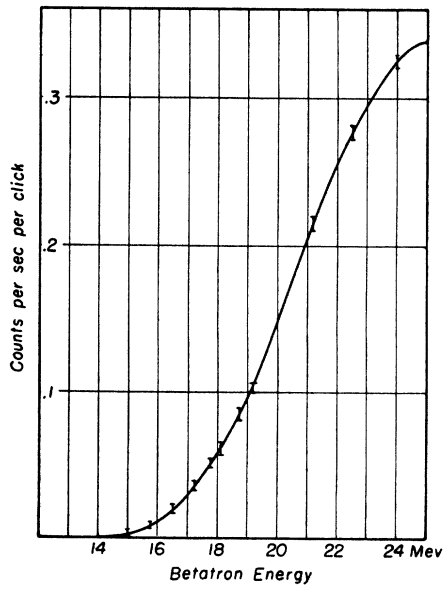

FIG. 7. $Mg^{25}(\gamma,p)Na^{24}$ yield curve based on Na^{24} activity.

[18] Johns, Katz, Douglas, and Haslam, Phys. Rev. **80**, 1062 (1950). We are indebted to Professor Katz for sending us these curves before publication.

normal and enriched foils and the observed proton yields, we calculate the isotopic yields to be $y_{25}=1.74\times10^5$ protons/mole/roentgen and $y_{24}=2\times10^5$ protons/mole/roentgen. Although Mg^{24} has a higher proton threshold than Mg^{25}, it also has a higher neutron threshold to compensate. The Mg^{25} yield determines the ordinate scale of Fig. 8 to be 0.0896×10^{-26} cm^2 in absolute units. The peak cross section is then 0.0137 barn at 20.5 Mev, and the integrated cross section is 0.056 Mev-barn. The cross section at 17.5 Mev is 0.004 barn. The uncertainty in these cross sections is also estimated to be of the order of 50 percent.

IV. DISCUSSION

The cross section of 0.004 ± 0.002 barn observed for $Mg^{25}(\gamma,p)Na^{24}$ at 17.5-Mev photon energy can be compared with the measurements of Hirzel and Wäffler[1] on the Na^{24} radioactivity produced by the lithium gamma-rays. They give a ratio of $Mg^{25}(\gamma,p)$ to $Cu^{63}(\gamma,n)$ of 0.0283 ± 0.0030. Using a cross section for $Cu^{63}(\gamma,n)$ at 17.5 Mev of 0.10 barn[18] gives for $Mg^{25}(\gamma,p)$, 0.0028 barn. The yield of protons from the normal magnesium, 18.6×10^4 protons/mole/roentgen, is about one-third that observed by Mann and Halpern[19] with a scintillation detector at 23.5-Mev betatron energy, but this difference is within the sum of the uncertainties. If we were to use Mann and Halpern's normal magnesium proton yield, the y_{24} would be about three times as great and the y_{25} about two-thirds the value we have calculated. Using our yields, 88 percent of the protons from the enriched foil are from $Mg^{25}(\gamma p)$; using Mann and Halpern's value, 60 percent from the enriched foil are from Mg^{25}. For the normal magnesium foil, the corresponding values of the protons produced by $Mg^{24}(\gamma,p)$ are 84 and 96 percent.

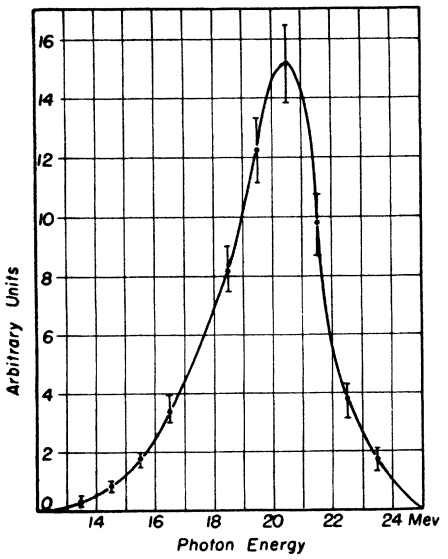

FIG. 8. Calculated relative cross-section curve for $Mg^{25}(\gamma,p)Na^{24}$ as a function of photon energy.

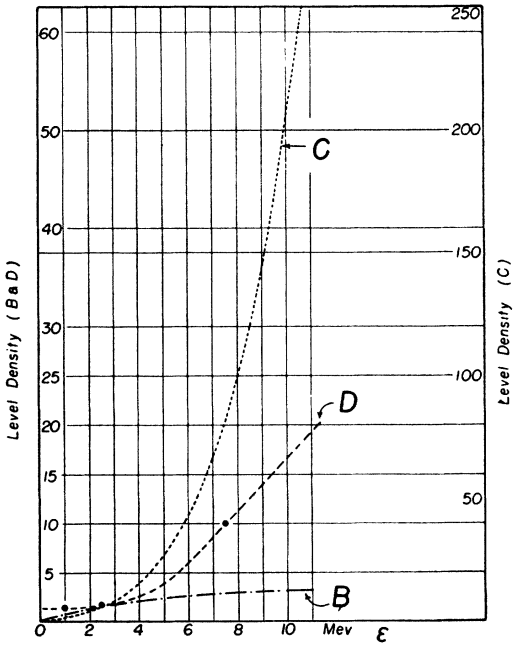

FIG. 9. Assumptions as to the energy level density of the resultant nucleus Na^{24}: curve B—ω_R from Schiff's formula, curve C—ω_R from Weisskopf and Ewing's formula, curve D—ω_R from Na^{24} levels.

Although the statistical model is not usually applicable in detail to such a light nucleus as magnesium, the calculation of the expected proton energy distribution is aided by the heterogeneous energy of the x-rays, which tends to average out the details of the level structure. Weisskopf and Ewing[2] give the distribution in energy ϵ of the protons from a nucleus b which has absorbed a photon of energy E as

$$I(\epsilon)=\text{const}\ \epsilon\, S_b(\epsilon)\xi_b\omega_R(E-E_b-\epsilon),$$

where ω_R is the level density of the resultant nucleus, ξ_b is the sticking factor (assumed to be unity), S_b is the coulomb penetration factor taken from tables,[20] and E_b is the binding energy of the proton. A distribution curve, I, is calculated for each E and normalized to the product of the 24-Mev bremsstrahlung curve and the relative cross-section curve at that E. The curve resulting from the addition of these I curves is normalized to the number of protons observed and compared to the observed proton energy distribution. Such a curve was calculated for each of several level density formulas. The assumed level densities of the resultant nucleus Na^{24} are plotted in Fig. 9 as a function of resultant nucleus excitation energy $\mathcal{E}=E-E_b-\epsilon$. Curve B is plotted from Schiff's formula[6] $\omega_R=(1/a)\times\ln[(\epsilon_0-\epsilon+a)/a]$, where $a=20/A$. Curve C is the

[19] A. K. Mann and J. Halpern, Phys. Rev. 81, 318 (1951).

[20] We are indebted to Professor Weisskopf for providing us with the latest tables of these penetration factors.

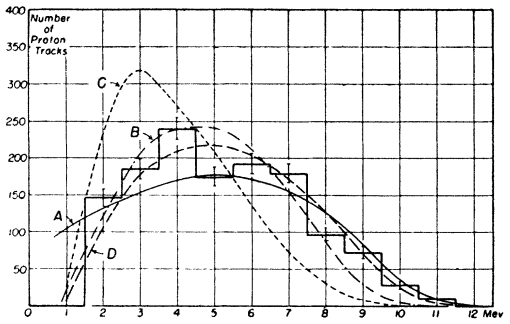

FIG. 10. Comparison of the observed photoproton energy distribution, shown by the histogram, with calculated curves: curve A—ω_R, a constant, curve B—ω_R from Schiff's formula, curve C—ω_R from Weisskopf and Ewing's formula, curve D—ω_R from Na^{24} levels.

statistical formula given by Weisskopf and Ewing[2] as $\omega_R = C \exp[a(E-E_b-\epsilon)]^{\frac{1}{2}}$, with $a=A/5$ and $C=0.2$ per Mev. Curve D is drawn from the known[21] levels of Na^{24}. The proton energy distributions calculated from these level densities are shown in Fig. 10 and compared with the observed proton energy distribution. The good agreement between the experimental curve and the curve D deduced from the known Na^{24} levels supports the concept of absorption of the photon energy into a compound nucleus with the subsequent evaporation of a proton (or a neutron). The uniformity of the angular distribution of the protons confirms this view. The observed integrated cross section of 0.056±Mev-barn can be compared with the values calculated on the dipole interaction. Goldhaber and Teller[7] estimate a total integrated photon absorption cross section of 0.36 Mev-barn for Mg^{25}. Price and Kerst[22] give 1.8×10^5 neutrons/mole/roentgen for normal magnesium photoneutron yield, much of which may be $Mg^{25}(\gamma,n)$ because of the high $Mg^{24}(\gamma,n)$ threshold. The sum of the $Mg^{25}(\gamma,p)$ and $Mg^{25}(\gamma,n)$ integrated cross sections seems smaller than, but may be consistent with, Goldhaber and Teller's value as well as Levinger and Bethe's[14] value of 0.52 Mev-barn for the integrated photon absorption. The resonance which is here observed at 20.5 Mev is predicted near 23.5 Mev on Goldhaber and Teller's picture and at about 29 Mev from Bethe and Levinger's calculations. There seems to be no major disagreement between these experiments, nor those of Diven and Almy on aluminum,[10] and the simple picture of photon absorption by dipole interaction, formation of a compound nucleus, and subsequent evaporation of neutrons and protons. In heavier nuclei, however, there seem to be anomalies[9,10,23] suggesting that occasionally the photoproton is ejected before its photoelectric energy is shared with the compound nucleus.[11] This may be the result of an increased nuclear mean free path at the higher energies available to the proton absorbing the photon because of lower proton binding energies. This can show up more easily in the heavier nuclei also because of the increased coulomb barrier which inhibits proton evaporation at the lower proton energies and consequently enhances the relative number of higher energy protons.

This research was supported in part by the joint program of the ONR and AEC. It was also aided by a grant from the Committee on the Advancement of Research of the University of Pennsylvania. The preparation of the enriched magnesium foil was accomplished by Mr. Victor Verbinski with the advice of Professor Knut Krieger of the Chemistry Department of the University of Pennsylvania. We appreciate the cooperation of the Isotopes Division of the AEC in the loan of the enriched magnesium.

[21] D. E. Alburger and E. M. Hafner, Revs. Modern Phys. **22**, 373 (1950).
[22] G. A. Price and D. W. Kerst, Phys. Rev. **77**, 806 (1950).
[23] P. R. Byerly, Jr., and W. E. Stephens, Phys. Rev. **81**, 473 (1951).